R. L. Gleason

S. P. Gray

Department of Biomedical Engineering,
Texas A&M University,
College Station, TX

E. Wilson

Department of Medical Physiology
and Cardiovascular Research Institute,
Texas A&M University System Health Science
Center,
College Station, TX

J. D. Humphrey[1]

e-mail: jhumphrey@tamu.edu
Department of Biomedical Engineering
and M.E. DeBakey Institute,
Texas A&M University,
College Station, TX

A Multiaxial Computer-Controlled Organ Culture and Biomechanical Device for Mouse Carotid Arteries

Much of our understanding of vascular mechanotransduction has come from studies using either cell culture or in vivo animal models, but the recent success of organ culture systems offers an exciting alternative. In studying cell-mediated vascular adaptations to altered loading, organ culture allows one to impose well-controlled mechanical loads and to perform multiaxial mechanical tests on the same vessel throughout the culture period, and thereby to observe cell-mediated vascular adaptations independent of neural and hormonal effects. Here, we present a computer-controlled perfused organ culture and biomechanical testing device designed for small caliber (50–5000 micron) blood vessels. This device can control precisely the pulsatile pressure, luminal flow, and axial load (or stretch) and perform intermittent biaxial (pressure–diameter and axial load–length) and functional tests to quantify adaptations in mechanical behavior and cellular function, respectively. Device capabilities are demonstrated by culturing mouse carotid arteries for 4 days. [DOI: 10.1115/1.1824130]

Keywords: Ex Vivo Perfusion, Organ Culture, Remodeling, Mechanical Properties, Vascular Smooth Muscle, Endothelium

Introduction

Cell-mediated growth and remodeling in arteries is controlled, in large part, via mechanosensitive responses by endothelial cells (EC), smooth muscle cells (SMC), and fibroblasts (FB) to altered loading: pulsatile pressure, flow, and axial load. The underlying mechanotransduction mechanisms play a fundamental role in many physiologic (e.g., normal vascular development) and pathophysiologic (e.g., hypertension, arteriosclerosis, and the development of aneurysms) processes, as well as in the success or failure of many clinical interventions (e.g., vein grafts, synthetic vascular grafts, stents, and balloon angioplasty). Although much of our understanding of vascular mechanotransduction has come from studies using cell cultures or in vivo animal models, the recent success of perfused organ culture systems offers an exciting alternative approach (e.g., Refs. [1–7]). Organ culture systems can provide a more tightly controlled mechanical environment compared to in vivo models, and can better maintain vessel geometry, structure, and cell-extracellular matrix attachments than cell culture techniques. In addition, organ culture can isolate the cell-mediated mechanisms of vascular adaptation by removing neural- and hormonal-induced mechanisms. EC and SMC function, comparable to that in control vessels, has been reported in cultured vessels for 6–9 days in large arteries [1,3,4,7] and up to 4 days in resistance arterioles [5]. In addition to the need to precisely control the loading, correlation of mechanically induced cellular responses to local alterations in mechanical loading necessitates sufficient information on the mechanical behavior of the tissue. Thus, if combined with biomechanical testing systems [8], organ culture offers the opportunity to perform multiaxial in vitro mechanical tests, at multiple time points of adaptation by the same vessel, that provide data sufficient to perform stress analyses and to develop mathematical models of growth and remodeling.

The aim of this work is to describe a novel computer-controlled organ culture device with biomechanical testing capabilities for the study of vascular adaptations in small caliber (50 to 5000 micron diameter) vessels. In addition to controlling the pulsatile pressure, luminal flow, and axial load (or stretch) throughout the culture period, this device enables intermittent biaxial (pressure–diameter and axial load–length) and functional tests to quantify adaptations in mechanical behavior and cellular function, respectively. Here, we illustrate capabilities of the device by culturing and testing mouse carotid arteries. We selected the common carotid artery because it is easy to excise with little dissection-induced damage, it is long, straight, and cylindrical with no branches, and the contralateral vessel provides a natural control for each animal. Indeed, reasonably priced ($\sim$\$27,000) paired devices allow both carotids to be tested in parallel. Thus, the carotids are well suited for ex vivo and in vitro tests. Our animal selection was motivated by the availability of genetic ''knockout'' models, which may allow future study of vascular adaptation wherein specific genes have been suppressed.

Device Development

There are many reports of the heart rate, blood flow, and blood pressure in mice (e.g., Refs. [9–15]). Reports vary due to many factors, including age, strain of mouse, and activity level (e.g., awake versus anesthetized, restrained versus unrestrained). Nevertheless, from these reports it appears that for a typical conscious, unrestrained, adult mouse, the mean heart rate is 5 to 11 Hz, the systolic and diastolic pressures are 120/80 mmHg, the mean arterial blood pressure is 93 mmHg, the mean volumetric blood flow through each carotid artery is 0.75 mL/min, and the peak systolic blood flow is 2.3 mL/min. A well-designed device should mimic these values. Because the viscosity of a typical culture media is 1 centipoise (cP), in contrast to $\sim$3.5 to 4 cP for the viscosity of blood, the perfused flow should be increased (i.e., 2.7–3.0 mL/min) to achieve the in vivo wall shear stress. We have assembled a computer-controlled device capable of accurately controlling mean vessel pressure up to 250 mmHg, mean flow rates up to 10.0 mL/min, pulse pressure magnitudes $>$40 mmHg at frequencies up to 15 Hz, and axial loads up to 10.0 grams (or stretches up to 2.5), while maintaining an adequate biochemical and physiological tissue culture environment. We describe the device in six functional units: the culture chamber, luminal pressure and flow control,

[1]To whom correspondence should be addressed.

Contributed by the Bioengineering Division for publication in the JOURNAL OF BIOMECHANICAL ENGINEERING. Manuscript received by the Bioengineering Division December 17, 2003; revision received June 8, 2004. Associate Editor: Michael Sacks

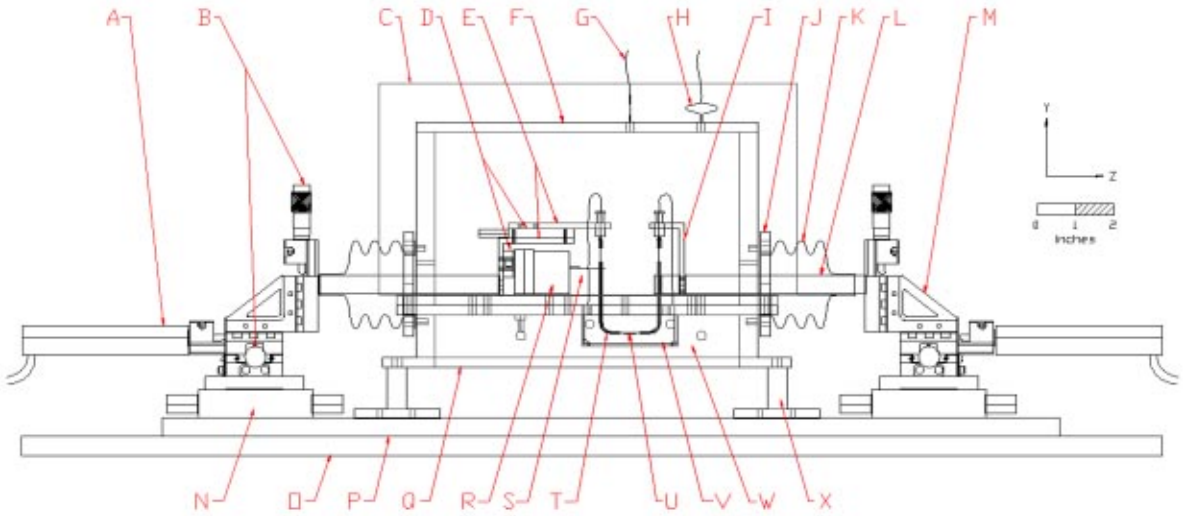

Fig. 1 Profile view of incubator chamber and mounting plate. See Table 1 for a detailed parts list.

axial loading and extension control, video imaging, the computer interface system, and physiologic (temperature, *p*H, humidity) control (see Figs. 1 and 2).

Culture Chamber. The custom chamber is designed to house a cannulated specimen as well as to control the temperature and *p*H in the adventitial bathing media and to provide a barrier to bacterial contamination while allowing long-term tissue culture on a laboratory bench top. The barrier is created by bolting a removable top (F) to the chamber (Q) and by sealing access holes on each end via flexible bellows (K) and bolted bellow mounts (J); silicone gaskets make each seal air tight. The isolated vessel is

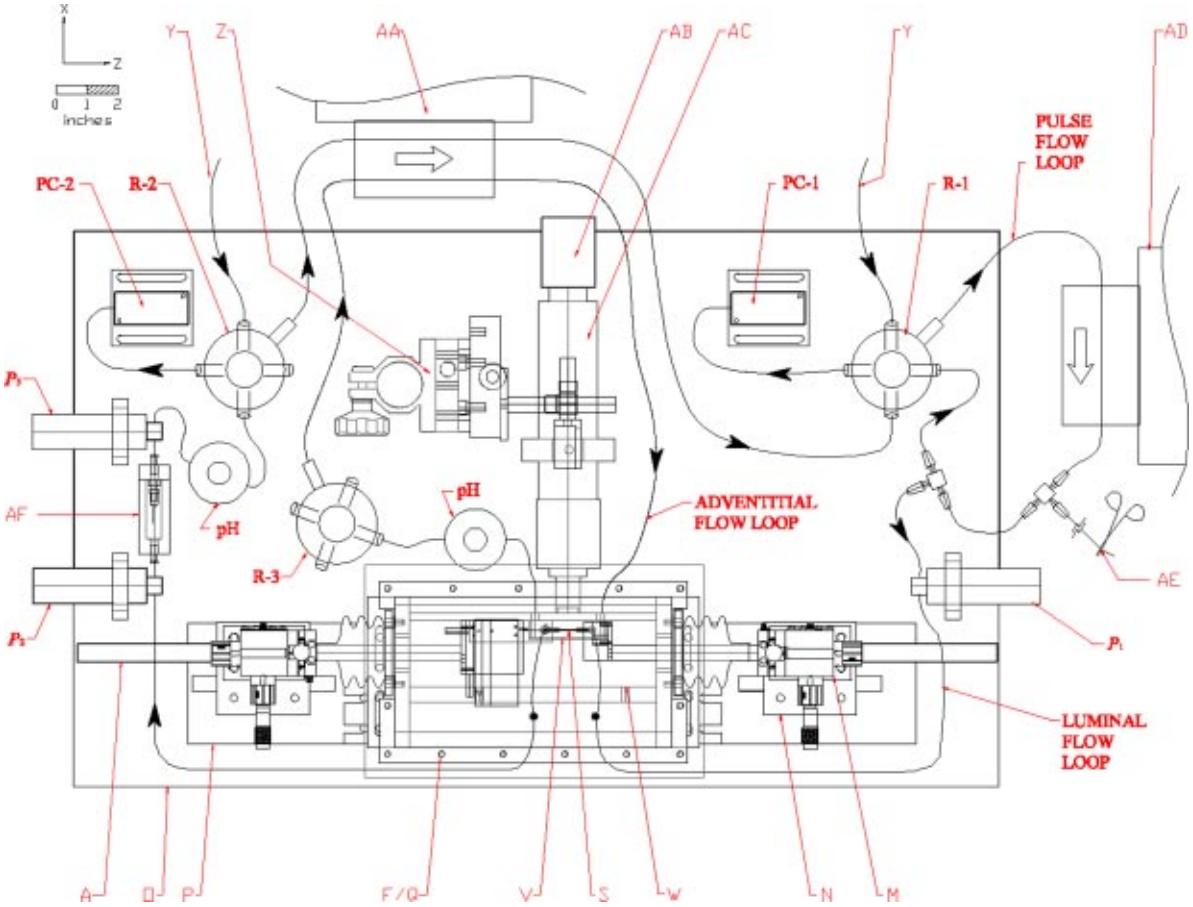

Fig. 2 Plan view of the overall organ culture and biomechanical testing device. See Table 1 for a detailed parts list.

mounted on custom glass cannulae (T) and connected to the stretching system via the access hole. Luminal flow enters the chamber through the top surface of the chamber via a threaded polypropylene luer fitting and connects to the cannula via a series of polypropylene fittings and Pharmed tubing. All components of the culture chamber are autoclavable. The 15-mL adventitial bath (V) is water-jacketed on four sides for temperature control; a fifth side is reserved for viewing/imaging the vessel.

Control of Luminal Flow and Pressure. A high-flow pulse-generation flow loop (Fig. 2) recirculates culture media via a peristaltic pump (AD) that is capable of generating pulse magnitudes >40 mmHg. The magnitude of the pulse pressure is controlled by positioning a hemostat along the length of a branching elastic tube (AE, following Ref. [3]). Luminal flow drawn from the pulse flow loop travels into pressure transducer P_1, into the culture chamber, through the vessel, out of the chamber, through P_2, through the custom flow meter (AF), through P_3, though the pH meter, and into the distal pressure control reservoir (R-2). By maintaining the pressure in two reservoirs (R-1 in the pulse flow loop, proximal to the vessel, and R-2 distal to the vessel), the mean luminal pressure and flow can be controlled independently. This is achieved by flowing a gas mix of 10% CO_2 in air through the reservoirs to the pressure controllers (PC-1 and PC-2); each pressure controller develops a backpressure, thus pressure is independently controlled in each reservoir. The mean vessel pressure P_v is approximated as $P_v = P_2 + k\Delta P_v$, where $\Delta P_v = P_1 - P_2$ and k is an empirical parameter. The mean flow rate is approximated as $Q = m\Delta P_f + b$, where $\Delta P_f = P_2 - P_3$ and m and b are determined via calibration; a custom flow chamber containing a small gauge needle between P_2 and P_3 is sized to provide an ~ 15 mmHg pressure drop at the desired flow rate, thus allowing sufficient resolution. Pumping media from reservoir R-2 back into R-1, via a second peristaltic pump (AA), completes the luminal flow loop. Note, too, that if only steady pressure and flow are desired, a simpler system can be used in which the entire pulse flow loop is removed, thereby allowing the mean pressure in the luminal flow loop to be controlled solely by R-2 and PC-2, with the flow rate (and thus pressure gradient) controlled by the peristaltic pump. Thus, for steady conditions, flow is recirculated from the distal reservoir through the pump, P_1, the vessel, P_2, the flow meter, P_3, pH meter, and then returned to the distal reservoir.

Axial Stretch/Load Control. The axial length of the vessel is controlled via two computer-controlled actuators (A) and the axial load is measured by a load cell (R). Each actuator is mounted to an XYZ stage (M), which in turn is mounted to a one-directional stage (N); along with the 1D stage, two manual micrometers (B) mounted on each XYZ stage allow positioning of each cannula during cannulation and ensure that the cannulae are parallel during setup. The stages are mounted on a removable stage plate (P) that rests on the base plate (O). The proximal cannula is clamped rigidly (to I), whereas the distal cannula is suspended from a cannula mount (E) via a compliant silicon tube and attached to the load cell via a custom wire hook (S). The distal glass cannula is joined to the wire hook with paraffin wax during system setup, which is easily removed postexperiment with local heating. Two micropositioners (D) allow movement of the load cell independent of the cannula and its mount, thus aiding in connecting and disconnecting the load cell hook from the cannula.

Stretch (defined as the loaded length divided by the unloaded length) is measured two ways: a mean stretch and a local stretch. The mean stretch is monitored by tracking the distance between the mounting sutures; this is achieved by monitoring the position of each actuator via the computer interface. The local stretch is monitored by tracking 20-μm-diameter microspheres that can be placed in a central region of the vessel (Fig. 3).

Imaging System. A video microscope (AC) and monochrome CCD (AB) allow continuous imaging of the vessel. Images are calibrated by viewing a grid of known dimension and generating a calibration curve for the horizontal and vertical directions. Since the video microscope is continuously focusable (to $8\times$), the focusing tube is locked prior to calibration and through the conclusion of each experiment. Viewing and focusing is achieved by translating the video microscope and CCD via the camera mount (Z). When viewing mouse carotid arteries, the vertical viewing field is set to ~ 840 microns; thus, for the 768×494 pixel CCD the resolution at this viewing field is ~ 1.7 micron/pixel. In addition to viewing the digitized images on the computer monitor, a B&W monitor and VCR allow monitoring and recording at a 60-Hz frame rate.

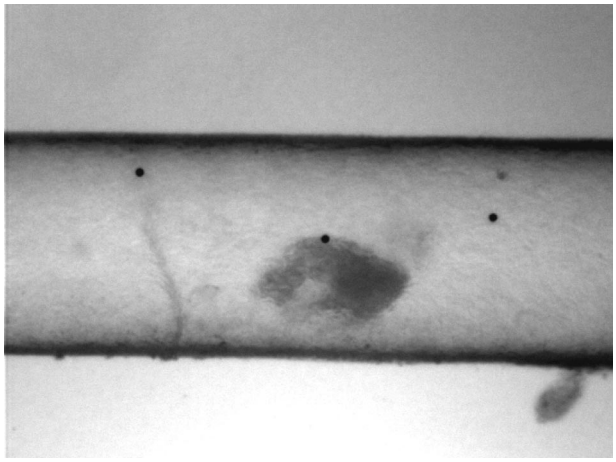

Fig. 3 Imaging of an isolated mouse common carotid artery with three 20-μm diameter video-tracking microspheres placed along the axis, which can be tracked in real time to monitor the local in-plane stretches. Here, $P_v = 93$ mmHg, $\lambda_z = 1.5$, and $Q = 0.75$ mL/min. Note that the vessel is translucent and the dark spot resulted from loose adventitia on the rear surface. The translucent character allows inner and outer diameter to be measured optically.

Computer Interface System. The analog components (i.e., P_1, P_2, P_3, PC-1, PC-2, pH meters, thermocouples, and axial load cell) interface with a desktop computer via a multifunction data acquisition (DAC) board. The CCD images are collected and digitized with an image acquisition board. The actuators are controlled via a motion control board, and a computer-controlled peristaltic pump is controlled via an RS-232 serial port. See Table 1 for hardware specifications.

A custom control program was written in LABVIEW 6.0 (National Instruments, Inc.) to control the vessel pressure (or circumferential stretch), flow rate, and axial load (or axial stretch) independently. LABVIEW IMAQ imaging software (National Instruments, Inc.) was employed to measure the vessel inner and outer diameter and to track the positions of the microspheres. A video-caliper subroutine allows the user to align arrows, superimposed on the image, with the inner and outer edges of the upper and lower wall, thereby manually measuring the inner and outer radii. The load is maintained by comparing the load cell output to a user-defined setpoint and tolerance; if the measured load is above the desired range, for example, the actuators are moved a user-defined increment so as to decrease the stretch (and load). Similar control–feedback loops were programed for pressure and flow control; the mean pressure is controlled by adjusting PC-1 and PC-2 in equal increments up or down, as necessary, whereas the flow is controlled by adjusting the difference (i.e., pressure gradient) between PC-1 and PC-2. The setpoints, tolerances, and increments for all control loops can be adjusted during program operation, thus allowing the user to define the control rate.

Data sampling from the DAC board is typically set at 1000 Hz. DAC values are averaged over a user-defined data collection pe-

Table 1 List of device components. NS=not shown.

Culture Chamber	
F	Incubation Chamber Top: Custom built polycarbonate, bolted, with silicone gaskets
J	Bellows Mount (2X): Custom polycarbonate
K	Flexible Neoprene Bellows (2X, McMaster-Carr)
Q	Incubation Chamber Bottom: Custom built polycarbonate, bolted, with silicone gaskets
V	Adventitial Bath
X	Chamber Mounts: Custom polycarbonate
Pulse, Luminal, and Adventitial Flow Loops	
PC-1, PC-2	Pressure Controller (2X, Alicat Scientific, PC-5PSIG-D/BP)
R-1, R-2, R-3	125 mL Erlenmeyer Flask (VWR), Customized with 5 Luer Ports
P_1, P_2, P_3	Pressure Transducer (0-5 psi, Sensotec, FPG)
Y	Gas Delivery Tubing (2X, Pharmed)
AA	Digital Pump Drive, Cartridge Pump Head and 2 Small Cartridges (Cole-Parmer)
AD	Variable Pump Drive and 3-Easy Load Pump Heads (Cole-Parmer)
AE	3-foot Silicon Tube with Hemostat Clamp
AF	Custom Flow-Through Cell with 26-Gauge Needle
Imaging System	
AB	Monochrome CCD (Sony, XC-ST50)
AC	Video Microscope (InfiniVar CFM)
Y	Camera Mount: (from left to right) Mounting Post, Clamp, and Y- Stage (Newport Corp., 40, 340-RC, and TSX-1D,), X-Stage and Posts (Edmunds Industrial Optics, E03-681 and L36-498), 90° Post Holder (Newport Corp., CA-1), and Aluminum Right Angle Bracket (Thor Labs, XE25A90)
NS	B&W Monitor (Sony)
NS	VCR (Panasonic)
Computer Interface	
NS	Desktop PC (Dell, Optiplex GX400)
NS	DAC Board: (Nat. Inst. PCI-6036)
NS	Frame Grabber (Nat. Inst. PCI-1407)
NS	Motion Control Board (Newport Corp., ESP6000)
Mounting and Axial Stretch/Load Control	
A	Computer-controlled Actuator (2X, Newport Corp., CMA-12CCCL)
B	Manual Micrometers (4X, Newport SM-13)
D	Micromanipulaters (2X, Newport MS-500)
E	Cannula/Load Cell Mounts: Custom aluminum
I	Cannula Mount: Custom aluminum
L	Stainless Steel Post (2X, Edmunds Industrial Optics, L36-499)
M	XYZ-Stage (2X, Newport Corp., M-461-XYZ)
N	1-D Stage (2X, Newport Corp., M-TSX-1D)
O	Aluminum Breadboard Plate (Newport Corp., SA-18"x30", ¼-20 threaded holes, 1" on-center)
P	Aluminum Stage Plate (Thor Labs, custom-built, 6"x24', M-6 threaded holes, 25-mm on-center)
R	5-gram Load Cell (Aurora Scientific, Model 400A)
S	Custom Hook for Axial Load Cell
T	Custom Cannula: 1-mm ID capillary tube (World Precision Instruments), with tips pulled to ~300 microns and notched for suture retention, bent at 90°, ½" from tip
U	Mouse Common Carotid Artery (CCA)
Temperature, pH, and Humidity	
pH	pH Meter with Flow-Through Cell (Lazar Laboratories)
C	Insulating Cover with Water-Jacket: Custom styrofoam, polycarbonate, and tygon tubing
G	Water-Jacketed Gas Delivery Tubing
H	0.2-Micron Filter (Wattman)
W	Water-Jacket for Adventitial Bath
NS	Temperature Control System: Temperature Controller (2X), Heater (2X) Thermocouple (3X): Cole-Parmer.
NS	Air Flow Controller (Alicat Scientific, 1 L/min)
NS	CO_2 Flow Controller (Alicat Scientific, 100 cm^3/min)

riod (typically 100 to 1000 ms) and a video image is collected (at a 30-Hz frame rate) and processed at the end of each data collection period. Mean values (over the data collection period) for pressures, input and output voltages from the pressure controllers, *p*H values, temperatures, and axial load, as well as the axial stretch, vessel outer diameter, maximum and minimum values of pressure (i.e., systolic and diastolic pressures), and acquisition time are written to a computer file. Data are typically stored every second, but this rate can be increased (up to 10 times per second) or decreased by the user; these data, along with the video-caliper data, can be stored by the user at any time. Waveform data (i.e., data at 1000 Hz) can also be collected and stored by the user at any time.

Control of pH, Temperature, and Humidity. A humid, temperature-controlled gas mixture of 10% CO_2 in air is continuously circulated though the free space within the culture chamber for *p*H and humidity control. The gas mix is bubbled through a 500-mL Erlenmeyer flask containing temperature-controlled, sterile, deionized water. The gas mix enters the Erlenmeyer flask through a 0.2-micron filter, then travels to the chamber via water-jacketed tubing (G), thereby maintaining temperature and humidity, and exits the chamber through a second 0.2-micron filter (H). Because the growth media used here is bicarbonate buffered, control of *p*H is achieved by maintaining an environment of 10% CO_2 in air. Note that the percentage of CO_2 in air can be adjusted from 0 to 20%, via an air- and a CO_2 flow controller (see Table 1), as needed.

Two independent temperature-controlled baths are recirculated via the peristaltic pump (AD) through the water-jacketing systems to maintain the temperature of the adventitial bath and the culture chamber. The temperature of each bath is maintained via an off-line temperature controller, heater, and thermocouple (see Table

1). The water from one bath is recirculated through the adventitial water jacket (W). The water from the other bath is recirculated though the water-jacketed tubing that supplies the gas mix to the chamber, then to a custom temperature-controlled insulating cover (C) that surrounds the walls of the chamber top, which minimizes heat loss. The insulating cover consists of an outer shell of Styrofoam, with ~10 ft of tygon tubing mounted in a meandering path along the inside surface to serve as a heat exchanger. Thermocouples can be placed in the adventitial bath, in the tubing providing luminal flow, and in the incubating chamber to confirm the temperature at these locations.

Experimental Methods

Surgical Preparation and Aseptic Setup. All system components that contact culture media were sterilized by autoclave, except for the pressure transducers and *p*H meters, which were thoroughly washed with 70% ethanol, rinsed with sterile water, and allowed to dry for 30 min within a laminar flow hood. Surgery and system assembly were also performed in a laminar flow hood. The three flow loops were assembled (with a by-pass where the incubating chamber will be), set in place on the bench top device, and *p*H and temperature control were initiated. The sterilized mounting components (posts/bellows, cannula mounts, cannula) were attached to the stages.

Wild-type adult male mice (FBV/N, Jackson Laboratories) were anesthetized with sodium pentobarbital (100 mg/kg IP) and heparinized (1000-unit/kg IP). Both mouse common carotid arteries were isolated, placed in fresh culture media, dissected free of perivascular tissue, and mounted on the cannulae using sterile 7-0 suture. The sterilized specimen chamber was set in place around the cannulated vessel, bolted and sealed, and the stage was set in place on the bench top device. The load cell was attached to the distal cannula and the flow loops and water-jacket tubing were connected to the chamber; perfusion was initiated gradually. The vessels were bathed and perfused with Dulbecco's modified Eagles medium (DMEM, Invitrogen, Inc., with 4500 mg/L D-glucose, L-glutamine, 110 mg/L sodium pyruvate, and pyridoxine hydrochloride), supplemented with 3.7 grams of sodium bicarbonate, antibiotic (P/S, Invitrogen, Inc., 1000 units/L of penicillin and 1000 g/L of streptomycin) and 0% to 20% heat-inactivated fetal bovine serum (HI-FBS, Hyclone). Typically, both carotids were cannulated (on separate devices) and subjected to experimental loading (luminal flow, pressure, and axial stretch) and physiological conditions (*p*H and temperature) within 2 h.

Flow Meter Calibration. Calibration curves were collected for 27-, 26-, and 23-gauge needles by maintaining ΔP_f at 5, 10, 15, 20, and 30 mmHg via computer control and by measuring the volumetric flow of culture media (DMEM+10% HI-FBS +1% P/S) over time; at least 35 mL of media were collected per calibration point.

Transmural Pressure. If P_v (calculated as $kP_1+(1-k)P_2$) is, indeed, the luminal pressure, then when P_v is maintained constant, the diameter of maximally dilated (i.e., noncontracting) vessels will also remain constant. Thus, the diameter of maximally dilated vessels (via administration of 10^{-4} M SNP) was monitored while flow was changed between 0 and 10 mL/min. To determine the true value of k for the system, the input value of k was adjusted iteratively until the diameter remained constant with constant pressure. Because much of the pressure drop occurs though the cannula, values of k from five different sets of cannula, with size-matched tips, were collected.

Functional Testing. Contractile function of the vessel was assessed at prescribed time points by observing the relative changes in diameter in response to the subsequent administration of three agents to the adventitial bath: phenylephrine (PE) to elicit smooth muscle cell contraction, acetylcholine (ACh) to elicit endothelial-dependent dilation, and sodium nitropruside (SNP) to elicit endothelial-independent dilation. By exchanging the adventitial media with new media containing the desired level of agonist, intermittent functional tests can be performed without breaching sterility.

Mechanical Testing. Under quasistatic conditions, pressure–diameter ($P-d$) and axial load–length ($f-\ell$) data were collected over 3 to 5 loading-unloading cycles for pressures of 0 to 160 mmHg at constant axial length, $\lambda_z^*=1.6$, 1.8, and 2.0, or over cyclic axial lengths up to $\lambda_z^*=2.0$ at constant pressures, $P_v=60$, 100, and 140 mmHg; here, $\lambda_z^*=\ell(s)/L(0)$, where $\ell(s)$ is the current (i.e., at growth and remodeling time s, measured in days) mean loaded axial length, and $L(0)$ is the initial unloaded diameter (at time $s=0$), collected at device startup. The current unloaded length was measured and the load offset was checked and adjusted (as necessary) before the $P-d$ tests and before and after the $f-\ell$ tests. At the end of the mechanical testing at each time s, the video-caliper subroutine was used to measure the inner and outer diameter of the vessel in ten configurations: $P_v=0$ and $\lambda_z^*=1.2$, 1.4, 1.6, and 1.8; $P_v=40$ and $\lambda_z^*=1.4$, 1.6, and 1.8; $P_v=80$ and $\lambda_z^*=1.6$ and 1.8; and $P_v=100$ and $\lambda_z^*=1.8$. In each of the ten configurations, given the measured inner and outer diameter and length measurements, the volume was calculated as $V=\pi(b^2-a^2)\ell$, where a and b are the inner and outer radii (equal to $\frac{1}{2}$ the measured inner and outer diameter), respectively; the reported volume $\overline{V}$ was the mean of the ten calculated V values. This measure of volume, combined with the outer diameter and total length measured during the $P-d$ and $f-\ell$ tests, was used to calculate the luminal radius over the testing cycles as $a=\sqrt{b^2-\overline{V}/(\pi\ell)}$ and the thickness as $h=(b-a)$, at each s. The mean circumferential stress (σ_θ) and axial stress (σ_z) were calculated as

$$\sigma_\theta=\frac{Pa}{h} \quad \text{and} \quad \sigma_z=\frac{f}{\pi(b^2-a^2)}.$$

The mean circumferential stretch was calculated, using the midwall radii $r_{\text{mid}}=(a+b)/2$ and $R_{\text{mid}}=(A+B)/2$, as $\lambda_\theta=r_{\text{mid}}/R_{\text{mid}}$ at each s and the axial stretch was calculated as $\lambda_z=\ell(s)/L(s)$.

Results

Flow and Pressure Calibration. There was little variation, between steady and pulsatile conditions, in the calibration curves for the mean flow rate for the needle sizes used (Table 2). For

Table 2 Calibration parameters for custom flow meter.

Needle size			Calibration parameters			
			Steady		Pulsed (+/−35 mmHg)	
Gauge	ID (μm)	Length (Inches)	m	b	m	b
27	203	0.5	0.021	−0.01	0.024	−0.08
26	254	0.5	0.045	0.01	0.044	0.00
23	432	1.5	0.132	0.06	0.134	0.04

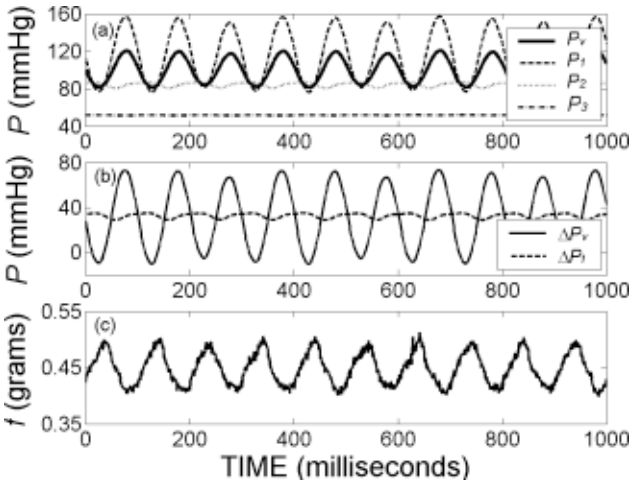

Fig. 4 (*a*) Pressure waveforms at various locations along the luminal flow loop. Notice that the vessel pressure, approximated as $P_v = P_2 + k\Delta P_v$ (where $\Delta P_v = P_1 - P_2$), ranges from 80 to 120 mmHg as desired. (*b*) Differential pressure waveforms ΔP_v and $\Delta P_f (= P_2 - P_3)$. (*c*) Axial load response to pulsatile pressure in (*a*).

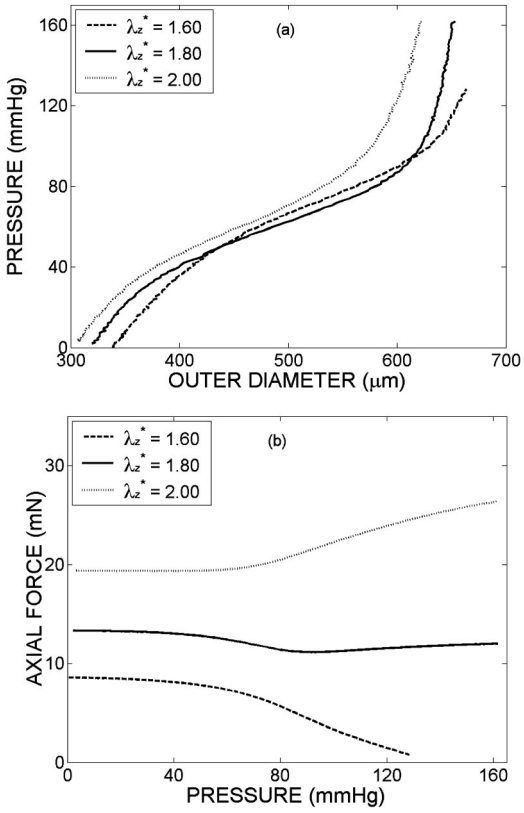

Fig. 6 (*a*) Pressure–diameter and (b) pressure–axial force curves during cyclic pressurization tests at fixed lengths on a freshly isolated mouse common carotid artery. Note the commonly observed force responses; see text.

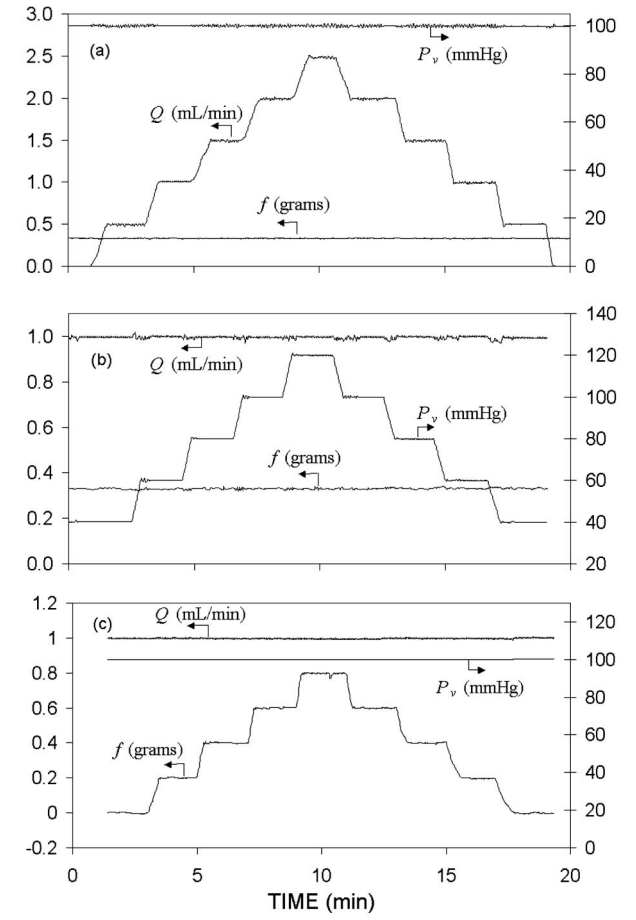

Fig. 5 Illustration of independent control of pressure, flow, and axial load. (*a*) Step changes in flow while maintaining constant pressure and axial load. (*b*) Step changes in pressure while maintaining constant flow and axial load. (*c*) Step changes in axial load while maintaining constant pressure and flow.

example, at $\Delta P_f = 15$ mmHg, the mean flow rates calculated from the calibration curves for steady and pulsatile conditions were 0.30 and 0.29 mL/min for the 27-gauge needle, 0.69 and 0.67 mL/min for the 26-gauge needle, and 2.04 and 2.05 mL/min for the 23-gauge needle, respectively. For sets of cannula with equally matched tips, the value of k was 0.5; that is, due to the symmetric design, an equal pressure drop occurs proximal and distal to the cannula, between P_1 and P_2.

Pulsatility. At a pulse frequency of 10 Hz (Fig. 4), the mean pressures were $\bar{P}_1 = 115.7$ mmHg, $\bar{P}_2 = 84.3$ mmHg, and $\bar{P}_3 = 51.7$ mmHg, with $\bar{P}_v = 100$ mmHg, and the mean differential pressures were $\Delta\bar{P}_v = 31.4$ mmHg and $\Delta\bar{P}_f = 32.6$ mmHg (note: for a flow meter needle that was $\frac{1}{2}$ in.-long and 26 gauge, $Q = 1.49$ mL/min). The pulse magnitudes were 80.8 (157/76.2) mmHg at P_1, 6.5 (88.1/80.6) mmHg at P_2, 0.4 (52.0/51.4) mmHg at P_3, and 39.3 (120.6/81.3) mmHg at P_v. The waveform of ΔP_v (an indicator of the magnitude and direction of flow through the vessel) varied from 73.3 to -10.3 mmHg (i.e., some reverse flow), whereas ΔP_f varied from 35.2 to 28.8 mmHg (i.e., no reverse flow). The axial load varied from 0.51 to 0.40 grams, with an average value of 0.45 grams. These data were collected for a passive, noncontracting vessel with $\lambda_z = 1.7$.

Loading Control. To illustrate the capability of independent control of loading (Q, P, and f), flow rate was incrementally increased, then decreased at user-defined values of 0.0, 0.5, 1.0, 1.5, 2.0, and 2.5 mL/min while holding the pressure and axial load constant. Similarly, pressure was incrementally increased, then decreased at user-defined values of 40, 60, 80, 100, and 120 mmHg, while holding the flow and axial load constant. Finally, axial load was incrementally increased, then decreased at user-defined values of 0.0, 0.2, 0.4, 0.6, and 0.8 grams while holding the flow and

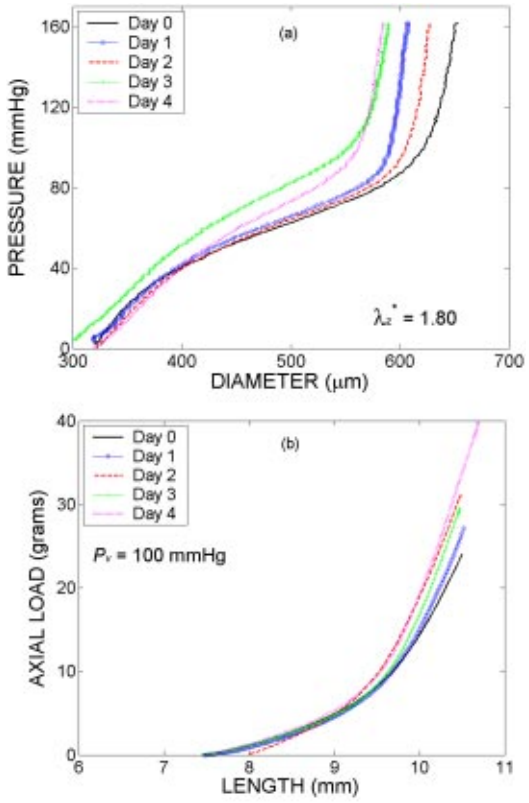

Fig. 7 (*a*) Pressure–diameter data from cyclic pressurization tests and (*b*) axial force–length data from cyclic extension tests at days 0, 1, 2, 3, and 4 during culture at P_v=100 ±20 mmHg (5 Hz), Q=0.50 mL/min, and λ_z^*=1.80.

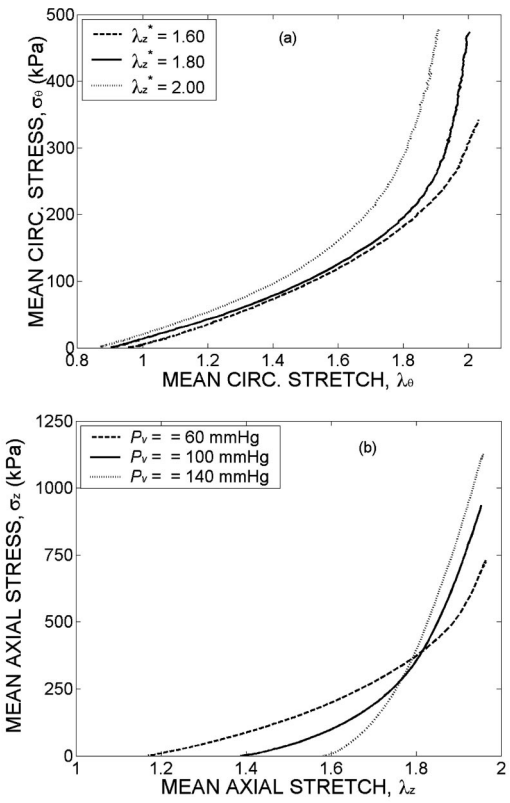

Fig. 8 Mean Cauchy stress–stretch data for (*a*) cyclic pressurization and (b) cyclic extension tests at multiple fixed axial stretches and luminal pressures, respectively. Data are from a control (day 0) vessel, with mean volume $\bar{V}$=0.270 mm^3, and unloaded length L=5.38 mm, diameter D=369 μm, thickness H=50 μm, and H:R_{mid}=0.31.

pressure constant. There were only small deviations in flow rate as the pressure was adjusted, and likewise for pressure as flow was adjusted (Fig. 5). We set the control-feedback increment values at 0.05 volts (1 volt=1 psi) for the pressure controller and 4 microns for the axial stretch control. Each step change (i.e., 20 mmHg pressure, 0.5 mL/min, or 0.2 grams) was achieved within 45 s of user command, remembering that our desired control is over hours to days; of course, different values of control–feedback increments will result in different response times. High values of control–feedback increments may cause the control parameter to overshoot the operation range, however, and to oscillate above and below this range. Note, too, that diameter (i.e., circumferential stretch) can be controlled (for steady pressure and flow conditions) rather than pressure, and axial length can be controlled rather than axial load. As an example of the latter, precise histories of cyclic stretching can be achieved at frequencies on the order of 1 Hz.

Functional and Mechanical Tests. Typical final loading curves (Figs. 6–8), plus unloaded length and thickness data, collected from a freshly isolated mouse common carotid artery, illustrate our ability to collect sufficient data to perform stress analyses. Notice the characteristic axial force response during P_v–d testing (Fig. 6), similar to that reported by many. That is, at low axial stretches the axial force decreases with increasing pressure, at high axial stretch the axial force increases with increasing pressure, and at near-in vivo stretch the axial force remains nearly constant with increasing pressure. These data can be collected at multiple time points throughout culture, with each vessel serving as its own control, thus allowing us to observe subtle changes in the character of the mechanical behavior (Fig. 7). Although many more tests are required to make statistically significant conclusions, note that, for this vessel, the outer diameter varied by more than 75 microns in the loaded configuration over the 4 days in culture. Clearly, one can only assume isochoric motions during intermittent testing.

Within 15 min of dosing with PE (10^{-5} M), the control vessel (i.e., within 2 h postsurgery) constricted to 72% of the original diameter and the vessel cultured for 4 days constricted to 73% of the initial diameter, with much of the constriction occurring in the first 5 min (Fig. 9). Following the addition of ACh (10^{-5} M), both vessels dilated to 84% of the initial diameter, but then both vessels constricted to 69% of the initial diameter. Addition of SNP (10^{-4} M) resulted in vessels dilated toward the initial diameters.

Discussion

It is well known that arteries tend to regulate lumen diameter in response to altered blood flow (e.g., [16]) and wall thickness in response to altered pressure (e.g., [17]). Recent observations similarly suggest that vessels grow and remodel in response to sustained changes in axial loading (e.g., [18]). Although we know that these adaptations result from mechanotransduction mechanisms, many of the associated details remain unclear. Our aim was to design a device to study mechanosensitive vascular growth and remodeling by imposing precise mechanical loads and chemical environments on small caliber, isolated blood vessels while measuring changes in functional and mechanical behaviors.

Vasoactivity is a major determinant of vessel caliber in response to acute changes in loading, and it plays an important role throughout growth and remodeling. Thus, it is essential to maintain ECs and SMCs in their native phenotypes throughout the culture period. Most investigators culture vessels in cell culture media (typically DMEM) with antibiotics and FBS, but the

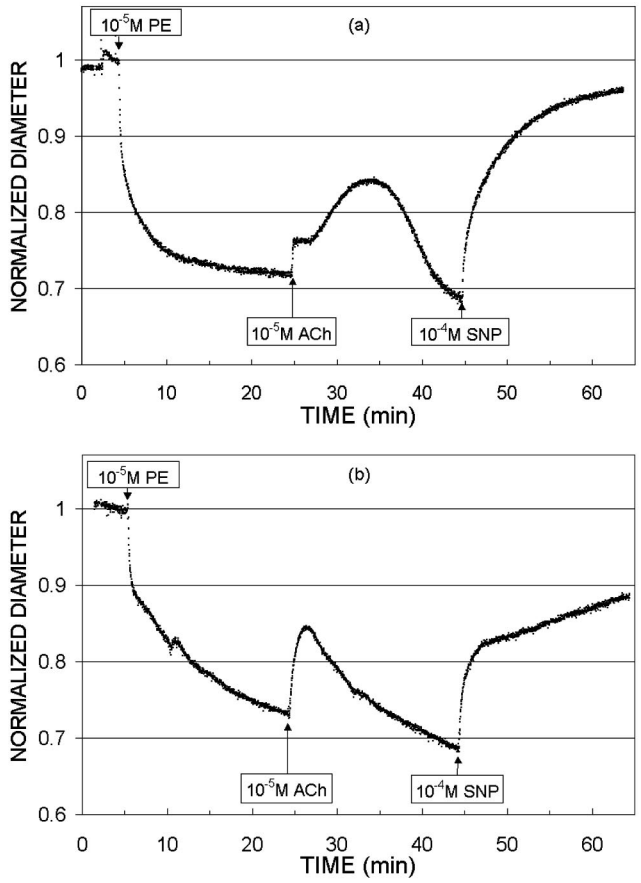

Fig. 9 Typical response to the administration of 10^{-5} M phenylehprine (PE), 10^{-5} M acetylcholine (ACh), and 10^{-4} M sodium nitropruside (SNP) in (*a*) freshly isolated and (*b*) 4-day cultured vessels. Note: vessel cultured at $P_v = 60$ mmHg (steady), $Q = 0.75$ mL/min, $\lambda_z = 1.65$.

amount of serum varies from study to study and functional response varies from animal to animal. We observed that, for mouse carotid arteries cultured in 10% HI-FBS, vessel response to PE, ACh, and SNP was maintained up to 4 days; from 4 to 6 days, response to ACh was gradually reduced, while SMC response to PE and SNP was maintained similar to control values (not shown). We observed similar results when cultured in 5% to 20% HI-FBS and when reducing the level of serum 5% per day from 20% to 5% and maintaining 5% thereafter (not shown). Mangiarua et al. [19] reported SMC function in a rat thoracic aorta at 3 and 6 days when cultured with Leibovitz L-15 medium and 10% horse serum, yet the endothelium was lost and SMC function was reduced compared to freshly isolated controls. Porcine common carotid arteries have been cultured in DMEM with 10% FBS and, although initially there is little response to agonists, vasoreactivity is present at 6 h and is maintained for 7 to 9 days [4,7,20]. Matsumoto et al. [4] showed vessel response to 100-mM KCl in rabbit carotid arteries cultured for 6 days in DMEM with 20% FBS (in a device adapted from Ref. [1]), but they reported a reduced response compared to controls. Labadie et al. [2] reported constriction of canine carotid arteries to epinephrine at 3 days and dilation to ACh at 2 days when cultured in medium 199 with 10% FBS. In small caliber vessels, Bakker et al. [5] presented a pressurized culture system (with very low flow) for rat cremaster arterioles cultured in DMEM with bovine serum albumin (BSA), HI-FBS, or dialyzed HI-FBS and showed responses to substance-P and serotonin at 4 days in the vessels cultured with HI-FBS and dialyzed HI-FBS, but ACh response was gradually lost, with no response by day 4; vessels cultured with BSA showed gradual loss of both endothelial-dependent dilators tested, with complete loss by day 4. Boltz et al. [6] reported responses to norepinephrine, ACh, and SNP at 2 days in hamster skeletal resistance arteries cultured in L-15 with 15% HI-FBS. Kim et al. [21] maintained contractility for 4 days in ferret aortic strips cultured in a cocktail of physiologic saline, DMEM, and antibiotics, with no serum; in fact, they show that contractility is lost when cultured in the presence of serum. Finally, Lemarie et al. [22] and Lehoux et al. [23] reported cultured mouse carotid arteries for 1 day and 3 days, respectively, but no functional tests were preformed. Clearly, the specific biochemical environment required to maintain vasoreactivity depends, at least in part, on the animal model, vessel location, and loading environment.

We employed computer control to maintain precise, long-term mechanical loading and testing. We modeled our biomechanical testing device after that of Humphrey et al. [8], wherein computer-controlled multiaxial mechanical tests were performed on large caliber vessels. Vorp et al. [24] extended the capabilities of this device to include long-term computer-controlled culture of large vessels, which provided much guidance for the development of our system. Guidance was also gained from Gan et al. [25], who also reported a computerized biomechanical perfusion device for large arteries. Note, too, that Faury et al. [26,27] reported pressure–diameter relations for freshly isolated mouse carotid arteries in wild-type and ELN+/− mice using a pressure arteriograph, and Lehoux et al. [24] reported pressure-diameter curves for normal and MMP-9 knockout mice at 0 and 3 days. Data from wild-type animals concur with our pressure-diameter results, but they did not collect axial load–length data.

A particular challenge when testing mouse arteries is the need for a high-frequency physiologic pulse wave at a low flow rate. In some systems for large vessels (and thus larger flow rates), pulse pressure is generated via a peristaltic pump (e.g., Refs. [1,3,28]). Alternatively, Moore et al. [29] generated physiologic pulse waves (at a flow of ~500 mL/min) by sending a voltage waveform to a computer-controlled gear pump. Still others have generated physiologic pulse waves via piston driven pumps. Brant et al. [30], for example, described a custom cam-driven piston pump capable of generating physiologic pulse waveforms at flows of 30–300 mL/min at 1–2 Hz. It appears, however, that none of these systems is capable of independent control of pulse frequency and flow rate (note: peristaltic pumps can operate at different flow rates at the same pulse frequency by using different tubing sizes, but these are incremental changes). Also, in scaling these systems from ~200 mL/min at 1 Hz to our desired flow rate of 0.1 to 10 mL/min at 5–15 Hz, the pulse generated by the peristaltic pump was significantly reduced (~3 mmHg or less in magnitude). Our system uses a high-flow pulse generation flow loop that takes advantage of the high magnitude and frequency of pulsatility that can be generated in previously reported systems, but achieves very low luminal flow by drawing only a portion (controllable) of the flow from the high-flow pulsed loop. Although we employ a peristaltic pump in the pulse generation flow loop (FL-1), any approach mentioned above (e.g., piston, bladder, or gear pumps) could be employed, perhaps providing more control over the shape of the pulse waveforms.

Finally, it has been proposed that arterial growth and remodeling tends to restore all stresses to near-homeostatic values [31–33], not just individual components in special cases. Unfortunately, most culture studies alter pressure or flow at a single fixed extension to observe changes in circumferential mechanical behavior, without consideration of alterations in axial loading. If mechanotransduction mechanisms and subsequent growth and remodeling are, in fact, triggered by local, multiaxial mechanical loading, then such data are incomplete. That is, at a minimum, one must have pressure–diameter and axial load–length data, and

(assuming incompressibility during mechanical testing) information on the wall thickness in at least one configuration to perform stress analyses [34].

In summary, we have designed and tested a computer-controlled vascular organ culture device capable of intermittent functional and biaxial mechanical testing of small caliber arteries. Such a device allows simultaneous study of cell signaling, contractile function, and mechanical behavior. In addition, this device provides another tool to study vessels from ''knockout'' mice. Thus, this device promises to provide new insights into mechanically induced vascular growth and remodeling.

Acknowledgments

This research was supported by a grant from the NSF (BES-0084644). We also acknowledge expert assistance from Jan Patterson, Dr. Michael Davis, and Dr. Lih Kuo, the Texas A&M University Chemistry Department glass blowers, and three Biomedical Engineering Students: Ruchi Singal, Charles Gordon, and Wendy Watson.

References

[1] Bardy, N., Karillon, G. J., Merval, R., Samuel, J.-L., and Tedgui, A., 1995, ''Differential Effects of Pressure and Flow on DNA and Protein Synthesis and on Fibronectin Expression by Arteries in a Novel Organ Culture System,'' Circ. Res., **77**, pp. 684–694.

[2] Labadie, R. F., Antaki, J. F., Williams, J. L., Katyal, S., Ligush, J., Watkins, S. C., Pham, S. M., and Borovetz, H. S., 1996, ''Pulsatile Perfusion System for Ex Vivo Investigation of Biochemical Pathways in Intact Vascular Tissue,'' Am. J. Physiol., **270**, (Heart Circ. Physiol. 39), pp. H760–H768.

[3] Chestler, N. C., Conklin, B. S., Han, H.-C., and Ku, D. K., 1998, ''Simplified Ex Vivo Artery Culture Techniques for Porcine Arteries,'' Annu. Rep. Prog. Chem., Sect. C: Phys. Chem., **4**, pp. 123–127.

[4] Matsumoto, T., Okumura, E., Miura, Y., and Sato, M., 1999, ''Mechanical and Dimensional Adaptation of Rabbit Carotid Artery In Vitro,'' Med. Biol. Eng. Comput., **37**, pp. 252–256.

[5] Bakker, E. N. T. P., van der Meulen, E. T., Spaan, J. A. E., and VanBavel, E., 2000, ''Organoid Culture of Cannulated Rat Resistance Arteries: Effect of Serum Factors on Vasoactivity and Remodeling,'' Am. J. Physiol., **278**, pp. H1233–H1240.

[6] Bolz, S.-S., Pieperhoff, S., de Wit, C., and Pohl, U., 2000, ''Intact Endothelial and Smooth Muscle Function in Small Resistance Arteries after 48 h in Vessel Culture,'' Am. J. Physiol., **279**, pp. H1434–H1439.

[7] Clerin, V., Nichol, J. W., Petko, M., Myung, R. J., Gaynor, J. W., and Gooch, K. J., 2003, ''Tissue Engineering of Arteries by Direct Remodeling of Intact Arterial Segments,'' Tissue Eng., **9**, pp. 461–472.

[8] Humphrey, J. D., Kang, T., Sakarda, P., and Anjanappa, M., 1993, ''Computer-aided Vascular Experimentation: A New Electromechanical Test System,'' Ann. Biomed. Eng., **21**, pp. 33–43.

[9] Hartley, C. J., Michael, L. H., and Enthman, M. L., 1995, ''Noninvasive Measurement of Ascending Aortic Blood Velocity in Mice,'' Am. J. Physiol., **268**, pp. H499–H505.

[10] Farrehi, P. M., Ozaki, C. K., Carmeliet, P., and Fay, W. P., 1998, ''Regulation of Arterial Thrombolysis by Plasminogen Activator Inhibitor-1 in Mice,'' Circulation, **97**, pp. 1002–1008.

[11] Transonic Systems, Inc., 1997, ''Tools and Techniques for Hemodynamic Studies in Mice,'' Available at http://www.transonic.com.

[12] Rudic, R. D., Bucci, M., Fulton, D., Segal, S. S., and Sessa, W. C., 2000, ''Temporal Events Underlying Arterial Remodeling after Chronic Flow reduction in Mice. Correlation of Structural Changes with a Deficit in Basal Nitric Oxide Synthesis,'' Circ. Res., **86**, pp. 1160–1166.

[13] Sullivan, C. J., and Hoying, J. B., 2002, ''Flow-dependent Remodeling in the Carotid Artery of Fibroblast Growth Factor-2 Knockout Mice,'' Arterioscler., Thromb., Vasc. Biol., **22(7)**, pp. 1100–1105.

[14] Gross, V., and Luft, F. C., 2003, ''Exercising Restraint in Measuring Blood Pressure in Conscious Mice,'' Hypertension, **41**, pp. 879–881.

[15] Li, Y.-H., Reddy, A. K., Taffet, G. E., Michael, L. H., Entman, M. L., and Hartley, C. J., 2003, ''Doppler Evaluation of Peripheral Vascular Adaptations to Transverse Aortic Banding in Mice,'' Ultrasound Med. Biol., **29**(9), pp. 1281–1289.

[16] Langille, B. L., Bendeck, M. L., and Keeley, F. W., 1989, ''Adaptations of Carotid Arteries of Young and Mature Rabbits to Reduced Carotid Blood Flow,'' Am. J. Physiol., **256**, (Heart Circ. Physiol. 25), pp. H931–H939.

[17] Matsumoto, T., and Hayashi, K., 1994, ''Mechanical and Dimensional Adaptation of Rat Aorta to Hypertension,'' ASME J. Biomech. Eng., **116**, pp. 278–283.

[18] Jackson, Z. S., Gotlieb, A. I., and Langille, L., 2002, ''Wall Tissue Remodeling Regulates Longitudinal Tension in Arteries,'' Circ. Res., **90**, pp. 918–925.

[19] Mangiarua, E. I., Moss, N., Lemke, S. M., McCumbee, W. D., Szarek, J. J., and Gruetter, C. A., 1992, ''Morphological and Contractile Characteristics of Rat Aortae Perfused for 3 and 6 Days In Vitro,'' Artery, **19**, pp. 14–38.

[20] Han, H.-C., and Ku, D. N., 2001, ''Contractile Response in Arteries Subjected to Hypertensive Pressure in Seven-day Organ Culture,'' Ann. Biomed. Eng., **29**, pp. 467–475.

[21] Kim, I., Je, H.-D., Gallant, C., Zhan, Q., Va Riper, D., Badwey, J. A., Singer, H. A., and Morgan, K. G., 2000, ''Ca^{2+}-Calmodulin-dependent Protein Kinase II-Dependent Activation of Contractility in Ferret Aorta,'' J Physio., **256, 2**, pp. 367–374.

[22] Lemarie, C. A., Esposito, B., Tedgui, A., and Lehoux, S., 2003, ''Pressure-induced Vascular Adaptation of Nuclear Factor-κB. Role of Cell Survival,'' Circ. Res., **93**, pp. 207–212.

[23] Lehoux, S., Lemarie, C. A., Esposito, B., Lijnen, H. R., and Tedgui, A., 2004, ''Pressure-induced Matrix Metalloproteinase-9 Contributes to Early Hypertension Remodeling,'' Circulation, **109**, pp. 1041–1047.

[24] Vorp, D. A., Severyn, D. A., Steed, D. L., and Webster, M. W., 1996, ''A Device for the Application of Cyclic Twist and Extension on Perfused Vascular Segments,'' Am. J. Physiol., **270**, (Heart Circ. Physiol. 39), pp. H787–H795.

[25] Gan, L., Sjogren, L. S., Doroudi, R., and Jern, S., 1999, ''A New Computerized Biomechanical Perfusion Model for Ex Vivo Study of Fluid Mechanical Forces in Intact Conduit Vessels,'' J. Vasc. Res., **36**, pp. 68–78.

[26] Faury, G., Maher, G. M., Li, D. Y., Keating, M. T., Mecham, R. P., and Boyle, W. A., 1999, ''Relation between Outer and Luminal Diameter in Cannulated Arteries,'' Am. J. Physiol., **277**, (Heart Circ. Physiol. 46), pp. H1745–H1753.

[27] Faury, G., Pezet, M., Knutsen, R. H., Boyle, W. A., Heximer, S. P., McLean, S. E., Minkes, R. E., Blumer, K. L., Kovacs, A., Kelly, D. P., Li, D. Y., Starcher, B., and Mecham, R. P., 2003, ''Developmental Adaptation of the Mouse Cardiovascular System to Elastin Haploinsufficiency,'' J. Clin. Invest., **112**, pp. 1419–1428.

[28] Niklason, L. E., Gao, J., Abbot, J. M., Hirschi, K. K., Houser, S., Marini, R., and Langer, R., 1999, ''Functional Arteries Grown In Vitro'' Science, **284**, pp. 489–493.

[29] Moore, J. E., Burki, E., Suciu, A., Zhao, S., Burnier, M., Brunner, H. R., and Meister, J.-J., 1994, ''A Device for Subjection Vascular Endothelial Cells to both Fluid Shear Stress and Circumferential Cyclic Stretch,'' Ann. Biomed. Eng., **22**, pp. 416–422.

[30] Brant, A. M., Chmielewski, J. F., Hung, T.-K., and Borovetz, H. S., 1986, ''Simulation In Vitro of Pulsatile Vascular Hemodynamics using a CAD/CAM-designed Cam Disc and Roller Follower,'' Artif. Organs, **10**, pp. 419–421.

[31] Taber, L. A., 1998, ''A Model of Aortic Growth based on Fluid Shear and Fiber Stresses,'' ASME J. Biomech. Eng., **120**, pp. 348–354.

[32] Rachev, A., 2000, ''A Model of Arterial Adaptation to Alterations in blood flow,'' J. Elast., **61**, pp. 83–111.

[33] Gleason, R. L., Taber, L. A., and Humphrey, J. D., 2004, ''A 2-D Model of Flow-induced Alterations in the Geometry, Structure, and Properties of Carotid Arteries,'' ASME J. Biomech. Eng., **126** pp. 371–381.

[34] Humphrey, J. D., 2002, *Cardiovascular Solid Mechanics: Cells, Tissues, and Organs*, Springer, New York.